Journal of Computational Design and Engineering, Vol. 1, No. 1 (2014) 27~36
www.jcde.org

Parametric surface and properties defined on parallelogrammic domain

Shuqian Fan*, Jinsong Zou and Mingquan Shi

Chongqing Institute of Green and Intelligent Technology, Chinese Academy of Sciences, Chongqing, China

(Manuscript Received September 8, 2013; Revised October 23, 2013; Accepted November 1, 2013)

Abstract

Similar to the essential components of many mechanical systems, the geometrical properties of the teeth of spiral bevel gears greatly influence the kinematic and dynamic behaviors of mechanical systems. Logarithmic spiral bevel gears show a unique advantage in transmission due to their constant spiral angle property. However, a mathematical model suitable for accurate digital modeling, differential geometrical characteristics, and related contact analysis methods for tooth surfaces have not been deeply investigated, since such gears are not convenient in traditional cutting manufacturing in the gear industry. Accurate mathematical modeling of the tooth surface geometry for logarithmic spiral bevel gears is developed in this study, based on the basic gearing kinematics and spherical involute geometry along with the tangent planes geometry; actually, the tooth surface is a parametric surface defined on a parallelogrammic domain. Equivalence proof of the tooth surface geometry is then given in order to greatly simplify the mathematical model. As major factors affecting the lubrication, surface fatigue, contact stress, wear, and manufacturability of gear teeth, the differential geometrical characteristics of the tooth surface are summarized using classical fundamental forms. By using the geometrical properties mentioned, manufacturability (and its limitation in logarithmic spiral bevel gears) is analyzed using precision forging and multi-axis freeform milling, rather than classical cradle-type machine tool based milling or hobbing. Geometry and manufacturability analysis results show that logarithmic spiral gears have many application advantages, but many urgent issues such as contact tooth analysis for precision plastic forming and multi-axis freeform milling also need to be solved in a further study.

Keywords: Spiral bevel gear; Mathematical modeling; Parametric surface; Geometrical characteristics; Manufacturability

1. Introduction

Parametric surfaces in computer aided geometric design (CAGD) are commonly defined on a triangular, rectangular or N-sided domain. The most important surface, the non-uniform rational B-spline (NURBS) surface, which is defined on a rectangular domain, is mainly used to describe the shape of industrial products. However, due to its intrinsic properties, the NURBS surface cannot accurately depict a class of kinematic or dynamic shape, such as the tooth surfaces of spiral bevel gears.

Spiral bevel gears, the teeth of which are curved and angled away from the shaft centerline, are widely used in the power transmission of intersection axes. Unlike spur and helical gears in which teeth are generated from a cylinder blank, in spiral bevel gears, teeth are generated on a conical surface, which allows the teeth to come into contact with each other gradually. Since these gears provide excellent smoothness and load capacity, they are one of the most essential components in modern mechanical engineering. Theoretically, the tooth surfaces of spiral bevel gears are spherical involute surfaces [1]; actually, the tooth flank geometry almost completely depends on the related cutting processes. More precisely, spiral bevel gears are manufactured using cradle-type milling or hobbing machine tools; their geometrical and functional properties are thus determined by the kinematic and dynamic characteristics of different machine tools. This is why standardized spiral bevel gears are not manufactured. Park and Lee [2] utilized the spherical involute tooth profile to standardize bevel gear systems and explained the geometric characteristics and kinematic behavior of the standardized bevel gears.

Based on the milling or hobbing process, several practical approaches have been taken [3-6] to design the tooth surface of a spiral bevel gear using NURBS. Since the tooth surface is constructed from actual tooth surface sampling points [3, 4] or machining simulation points [5, 6], in the final digital model, the parametric feature information such as spiral angle, nominal pressure angle, module, etc. is completely lost. The NURBS based approach cannot be conveniently used for the parametric modeling of a spiral bevel gear.

Computer numerical control (CNC) cradle-type machine

*Corresponding author. Tel.: +86 -23-6593-5572, Fax.: +86-23-6593-5416
E-mail address: fansq@cigit.ac.cn

doi: 10.7315/JCDE.2014.003

tools have made it possible to perform nonlinear correction motions for the pinion and gear tooth surface cutting. Thus, better tooth contact quality should be achieved by using the optimal settings of machine tools according to the tooth contact analysis (TCA) method [7-12]. Litvin et al. [8, 9] proposed a local synthesis of spiral bevel gears with localized bearing contact and the predesigned parabolic function of a controlled level for transmission errors. The pinion tooth surface is generated by roll modification and cutting ratio variation in the process. Cao et al. [10] developed a function-oriented active tooth surface design methodology to incorporate transmission errors and the contact path in the engagement process of the spiral bevel gears. Favorable shape could therefore be controlled directly before manufacturing with cradle-type machine tools. Tang et al. [11] considered the kinematical errors of machine tools and the installation errors of the gear pairs in TCA. In their proposed error tooth contact analysis (ETCA) method, more processing parameters should be recommended than in TCA in spiral bevel gears cutting. However, because tooth surface quality is very sensitive to the dynamic errors of cradle-type machine tools, cutting parameters adjustment for machine tools is time-consuming tedious work and is unavailable in most cases. Furthermore, due to the limited cutting processes, it is known that the spiral angle is not constant along the spiral bevel gear tooth. Consequently, Huston and Coy [13] believed that the inconstant spiral angle adversely modifies the tooth surface characteristics, which in turn greatly affects the load distribution, contact stress, and erratic kinematics, while inducing vibrations for the spiral bevel gears. In other words, an inconstant spiral angle cannot insure uniform kinematics and dynamics along the gear tooth with the mating gear.

The logarithmic spiral (also known as the equiangular spiral or growth curve), which commonly appears in nature, was first introduced into spiral bevel gear transmission for tooth surface description by Huston and Coy [13]. The logarithmic spiral bevel gear is considered to be an ideal spiral bevel gear due to its constant spiral angle properties. However, it is not convenient to manufacture such gears in the modern gear industry. Thus, a mathematical model suitable for accurate digital modeling and the differential geometrical characteristics of the tooth surface have not yet been thoroughly investigated. Tsai and Chin [14] applied the logarithmic spiral in bevel gear systems. They provided a relative complex mathematical description of the spiral tooth surface by solving equation systems. Hence, the surface representation does not have intuitive geometric meaning and is unsuitable for manufacturability analysis. Based on intuitive space geometry and kinematic theory, Li et al. [15] derived the spatial equation of the tooth surface. However, the form of the derived equation is difficult to understand without the help of professional tools such as CAD or Matlab platform. Recently, precision plastic forming processes, such as forging and cold extrusion have made it possible to mass produce small module spiral bevel gears that are widely used in the automobile industry [2, 16]. Meanwhile, general multi-axis CNC milling machine tools (rather than the special cradle-type machine tools), have also made it possible to manufacture high precision large module gears in small batches for the shipbuilding industry [2, 17].

This paper is divided into five sections. In Section 1, the most intuitive mathematical model for the tooth surface of the logarithmic spiral bevel gear is proposed. Section 2 discusses the unified parametric surface definition on the parallelogrammic domain for different kinematic styles. The differential geometrical characteristics which will be useful for understanding tooth geometry and its manufacturability are then explained in Section 3. The logarithmic spiral bevel gear manufacturability with precision plastic forming processes and multi-axis freeform surface milling processes is then analyzed in Section 4. Section 5 then presents a discussion of the application advantages and the many urgent issues that still need to be solved. Our main contributions are the unified parametric representation of the logarithmic spiral tooth surface, and the manufacturability analysis of the logarithmic spiral bevel gear with derived surface intuitive properties.

2. Tooth surface geometry

We focus on the most important factors that influence the configuration of an accurate mathematical model of the spiral bevel gear tooth surface. In order to meet a constant spiral angle transmission condition, we consider the logarithmic spiral curve in the tooth surface geometry.

2.1 Spherical involute

The spherical involute geometry is well described by Shunmugam et al. [18]. In addition, other works on the spherical involute geometry can be referred to [2, 14]. For ease of understanding Section 2.3, we illustrate the spherical involute geometry in this section as presented in [18].

The basic kinematic characteristics of a bevel gear pair may be described using the pitch cones and base cones. Un-

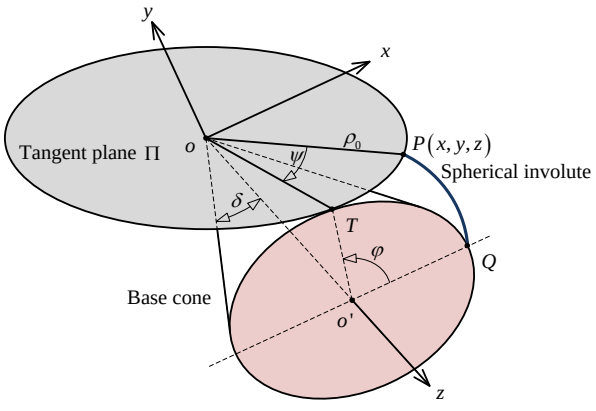

Figure 1. Spherical involute geometry.

folding the base cone surface, point Q on the generatrix of the surface will trace a spherical involute $P(x,y,z)$ as shown in Figure 1. In the right-handed coordinate system, assume that ρ_0 is the distance from the apex o to point Q and δ is the base cone angle. P is a point on the spherical involute curve generated by point $Q(\rho_0\sin\delta,0,0)$, and $T(\rho_0\sin\delta\cos\varphi, \rho_0\sin\delta\sin\varphi,0)$ is the tangent point on the base cone, where the involute generating angle φ is measured from $o'Q$ to $o'T$ on the base. The base cone surface can be formulated as

$$f(x,y,z) = x^2 + y^2 - z^2(\tan\delta)^2 = 0. \quad (1)$$

Unfolding and stretching the base cone surface, the cut off generatrix oQ will form a plane Π tangent to the base cone surface at the generatrix oT. A family of tangent planes will be obtained, while angle φ varies. The family of tangent planes, which envelopes the base cone, may be described by a single parametric equation as

$$\Pi(x,y,z,\varphi) = x\cos\delta\cos\varphi + y\cos\delta\sin\varphi - z\sin\delta = 0. \quad (2)$$

Also, the arc length QT should clearly be equal to PT; i.e., $\psi = \varphi\sin\delta$. Associated with the coordinate system, the chord length of PT can finally be formulated as

$$(x-\rho_0\sin\delta\cos\varphi)^2 + (y-\rho_0\sin\delta\sin\varphi)^2 + (z-\rho_0\cos\delta)^2 = 4\rho_0^2\sin^2(\psi/2) \quad (3)$$

using

$$x^2 + y^2 + z^2 = \rho_0^2. \quad (4)$$

Then, solving Eqs. (2)-(4) simultaneously, the location of P can be obtained as

$$\begin{cases} x = \rho_0(\cos\psi\cos\varphi\sin\delta + \sin\psi\sin\varphi) \\ y = \rho_0(\cos\psi\sin\varphi\sin\delta - \sin\psi\cos\varphi) \\ z = \rho_0\cos\psi\cos\delta \end{cases}. \quad (5)$$

Eq. (5) can be written as

$$\begin{bmatrix} x \\ y \\ y \end{bmatrix} = \begin{bmatrix} \cos\varphi & \sin\varphi & 0 \\ \sin\varphi & -\cos\varphi & 0 \\ 0 & 0 & 1 \end{bmatrix}\begin{bmatrix} \cos\psi & 0 & 0 \\ 0 & \sin\psi & 0 \\ 0 & 0 & \cos\psi \end{bmatrix} \times \begin{bmatrix} \rho_0\sin\delta \\ \rho_0 \\ \rho_0\cos\delta \end{bmatrix} = \boldsymbol{R}_\varphi\boldsymbol{R}_\psi\boldsymbol{V}_{\rho_0}. \quad (6)$$

2.2 Planar logarithmic spiral

Since every point on the logarithmic spiral has a constant spiral angle β between the tangent line and the radial line as shown in Figure 2, the planar logarithmic spiral is also called an equiangular spiral. Here, the local moving coordinate system $ox'y'z'$, which is used to depict the logarithmic spiral, is constructed on the tangent plane Π on the base cone, where o is the apex.

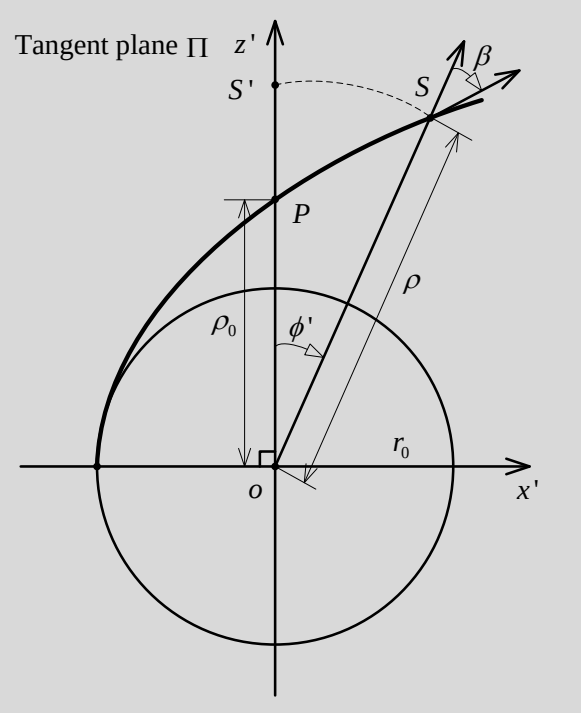

Figure 2. Planar logarithmic spiral.

The equation of the planar logarithmic spiral can by written with polar form as

$$\rho = r_0 e^{(\pi/2+\phi')\cot\beta} = r_0 e^{\phi'\cot\beta} \quad (7)$$

where r_0 is the radius of the base circle of the planar logarithmic spiral, and $\rho_0 = r_0 e^{(\pi/2)\cot\beta}$.

2.3 Planar logarithmic spiral

Take the local moving coordinate system $ox'y'z'$ into the global coordinate system $oxyz$. ox' axis coincides with the ox axis, and oz' axis coincides with the generatrix of the base cone as the kinematic initial condition, as shown in Figure 3. When the tangent plane Π rolls over the base cone without slipping, any point on the planar logarithmic spiral such as S can generate a trajectory after it contacts the base cone. Practically, the trajectory of S is a spherical involute, as described in section 2.1. When point S contacts the base cone, the contact point S can be taken as the coordinate transformation result in the case where a point S' (in Figure 2) positioned on the generatrix oQ rotates around the oz axis.

According to cone geometry relations, the rotation angle ϕ can be expressed as

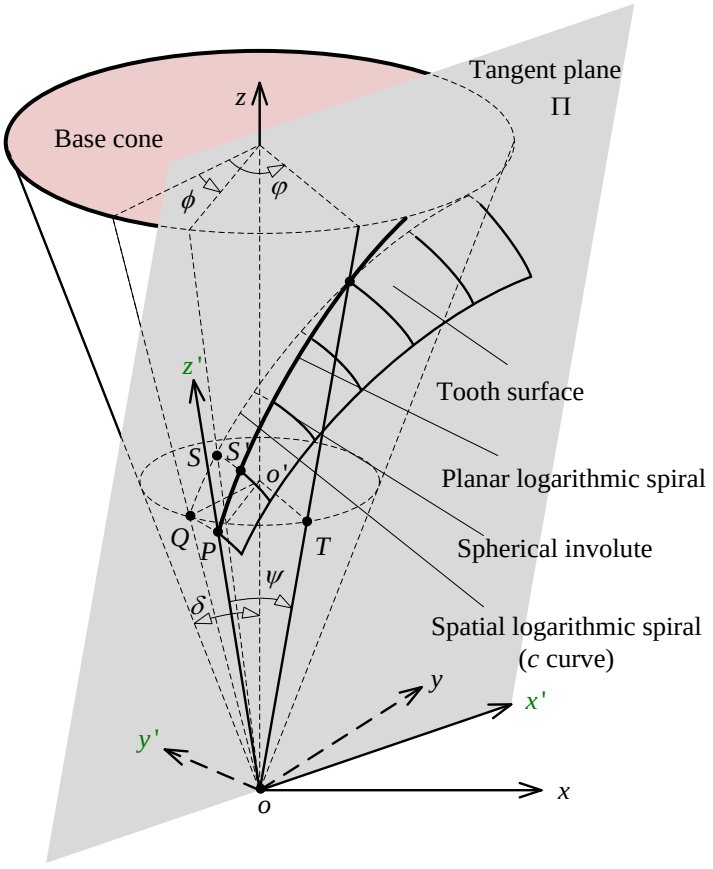

Figure 3. Tooth surface geometry.

$$\phi \sin\delta = \phi'. \tag{8}$$

Substituting the planar logarithmic spiral developing angle ϕ' with the rotation angle ϕ, Eq. (7) can be formulated as

$$\rho = \rho_0 e^{\phi \sin\delta \cot\beta}. \tag{9}$$

The rotation transformation of *S* is

$$\boldsymbol{R}_\phi = \begin{bmatrix} \cos\phi & -\sin\phi & 0 \\ \sin\phi & \cos\phi & 0 \\ 0 & 0 & 1 \end{bmatrix}. \tag{10}$$

Referring to Eq. (6), the variables related to the trajectory equation of *S* can be easily expressed as

$$\boldsymbol{R}_\phi = \begin{bmatrix} \cos(\varphi-\phi) & \sin(\varphi-\phi) & 0 \\ \sin(\varphi-\phi) & -\cos(\varphi-\phi) & 0 \\ 0 & 0 & 1 \end{bmatrix}, \tag{11}$$

$$\boldsymbol{R}_\psi = \begin{bmatrix} \cos\psi & 0 & 0 \\ 0 & \sin\psi & 0 \\ 0 & 0 & \cos\psi \end{bmatrix}, \tag{12}$$

and

$$\boldsymbol{V}_\rho = (\rho\sin\delta, \rho, \rho\cos\delta)^T \tag{13}$$

where $\psi = (\varphi - \phi)\sin\delta$. The trajectory of *S*, more precisely a spherical involute, can be formulated as a parametric equation of φ as

$$(x, y, z)^{\boldsymbol{T}} = \boldsymbol{R}_\phi \boldsymbol{R}_\varphi \boldsymbol{R}_\psi \boldsymbol{V}_\rho. \tag{14}$$

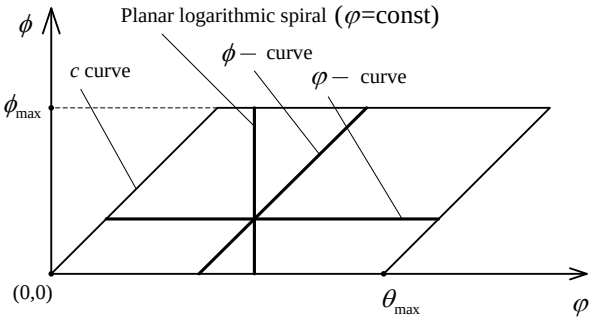

Figure 4. Parallelogrammic domain of tooth surface.

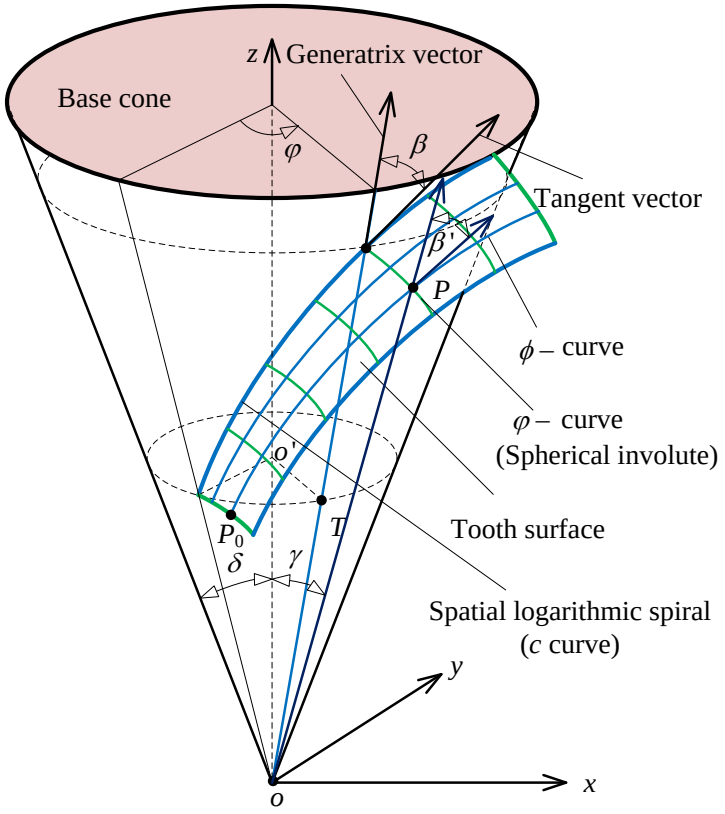

Figure 5. Tooth surface and its characteristics.

Since S can be an arbitrary point on a planar logarithmic spiral, the tooth surface expression $\boldsymbol{r}(\varphi,\phi)$ can be described with bi-parametric style in a natural way as

$$\boldsymbol{r}(\varphi,\phi) = \boldsymbol{R}_{\phi}\boldsymbol{R}_{\varphi}\boldsymbol{R}_{\psi}\boldsymbol{V}_{\rho}. \tag{15}$$

Eq. (14) can be rewritten in a coordinate components form as

$$\begin{cases} x(\varphi,\phi) = (\cos\psi\cos\varphi\sin\delta + \sin\psi\sin\varphi)\rho_0 e^{\phi\sin\delta\cot\beta} \\ y(\varphi,\phi) = (\cos\psi\sin\varphi\sin\delta - \sin\psi\cos\varphi)\rho_0 e^{\phi\sin\delta\cot\beta} \\ z(\varphi,\phi) = \cos\psi\cos\delta\,\rho_0 e^{\phi\sin\delta\cot\beta} \end{cases} \tag{16}$$

where $\psi = (\varphi-\phi)\sin\delta$, $0 \le \varphi-\phi \le \theta_{max}$, and $0 \le \phi \le \phi_{max}$. θ_{max} and ϕ_{max} are specified angle constraints that are related to the detailed parameters of the spiral bevel gear design.

Figure 4 expresses the parallelogrammic domain of the tooth surface, which differs somewhat from the rectangular domain of the classical freeform surface such as in B-spline and NURBS. When φ is equal to a constant, its mapping curve on the tooth surface is exactly the planar logarithmic spiral in the moving tangent plane Π (in Figure 3). Similarly, when ϕ is a constant, the mapping of the φ-curve is a spherical involute.

Meanwhile, the parallelogrammic domain can be taken as a result of the c curve sweep along the φ direction. Hence, without regard to the planar logarithmic spiral, the tooth surface can be considered as being generated by a spatial curve (c curve in Figure 3) on the base cone in geometrical view. When $\varphi - \phi = 0$, we have

$$c(\phi) = \rho_0 e^{\phi\sin\delta\cot\beta}(\cos\phi\sin\delta, \sin\phi\sin\delta, \cos\delta)^{\boldsymbol{T}}. \tag{17}$$

According to Eq. (17), the c curve is certainly a spatial logarithmic spiral [19]. The spatial logarithmic spiral also has a constant spiral angle β between its tangent vector and the generatrix vector, as seen in Figure 5. Figure 5 also illustrates the φ-curve (ϕ = constant) and the φ-curve (φ-ϕ = constant) on the tooth surface.

3. Unified parametric surface description

The above mentioned parametric surface equation is clearly derived from the clockwise direction of ϕ, which is the same direction as the spiral angle β (see Figure 2) and the counterclockwise direction of φ (from top view, see Figure 3). If we change any direction of φ or ϕ, we can harvest different

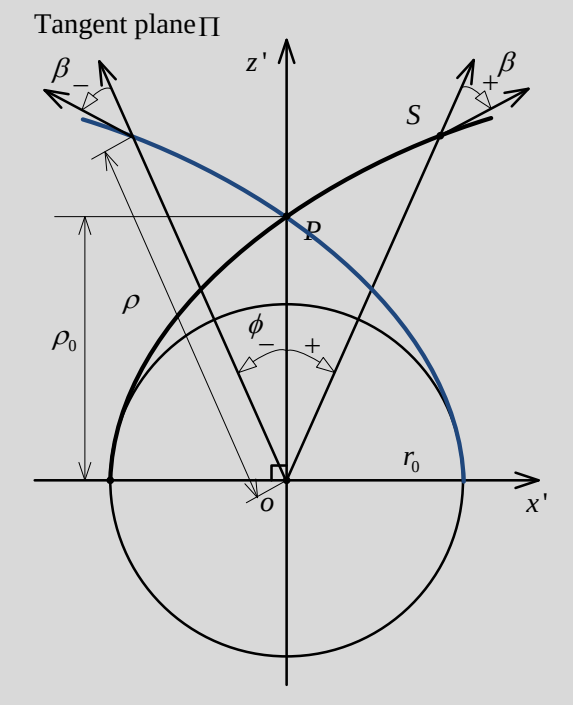

Figure 6. Planar spiral in different direction.

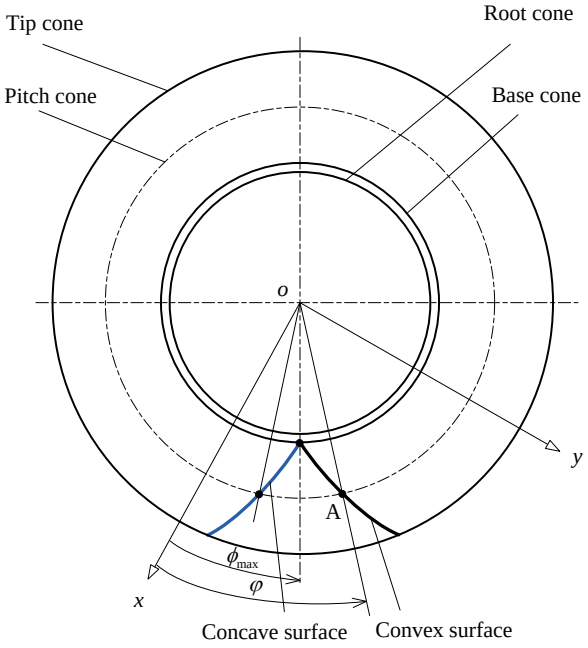

Figure 7. Planar spiral in different directions.

parametric surfaces that can be used for bevel gears design.

3.1 Unified description for planar spiral

The direction of the spiral angle β determines whether the gear tooth is left-hand or right-hand. In the left-hand/right-hand gear tooth, the outer half of the tooth is inclined in the counterclockwise/clockwise direction from the axial plane through the midpoint of the tooth, as viewed by an observer looking at the face of the gear.

Assume that the counterclockwise direction of spiral angle β is positive (-), and vice versa, as illustrated in Figure 6. The planar logarithmic spiral can then be formulated as

$$\rho = r_0 e^{(-\pi/2+\phi')\cot\beta} = \rho_0 e^{\phi'\cot\beta} \tag{18}$$

where $\rho_0 = r_0 e^{-\pi\cot\beta/2}$ and $\beta \le 0$, $\phi' \le 0$. Eq. (18) has the same style as Eq. (7); regardless of the direction of the spiral angle, the planar logarithmic spiral has a unified definition.

3.2 Convex/concave tooth surface

Obviously, Eq. (15) represents the convex tooth surface of different direction spiral bevel gears. Compared with the convex surface generating principle, the concave surface can be considered as the trajectory in which the logarithmic spiral curve in the tangent plane Π rolls over the base cone without slipping in the negative (-) direction (clockwise direction).

Consequently, the equation of the concave surface is the same as the convex surface equation. The difference is the definition domain of parameter φ, as shown in Figure 7.

3.3 Surface on parallelogrammic domain

According to the above analysis, we can depict the tooth surfaces using a unified parametric surface Eq. (15). All surfaces are defined on different parallelogrammic domains that depend on the direction of φ and ϕ. Figure 8 shows the category of the tooth surfaces.

4. Differential geometrical characteristics

The elastohydrodynamic lubrication, surface fatigue, contact stress, wear, life and manufacturability of the spiral bevel gears heavily rely on the differential geometrical characteristics of the tooth surface, such as normal vectors, principal curvatures and directions. The many advantageous properties of the logarithmic spiral bevel gears should be revealed by using classical differential geometry tools.

4.1 First fundamental form

The tooth surface Σ is described by a pair of parameters φ and ϕ through the vector equation $\boldsymbol{r}(\varphi,\phi)$, where $\boldsymbol{r}$ is the position vector of a typical point P on Σ. The base vectors of Σ at any point P are then given by

$$\frac{\partial \boldsymbol{r}}{\partial \varphi} = \rho \sin\psi \cos\delta \begin{bmatrix} \cos\varphi\cos\delta \\ \sin\varphi\cos\delta \\ -\sin\delta \end{bmatrix}, \tag{19}$$

and

$$\frac{\partial \boldsymbol{r}}{\partial \phi} = \frac{\rho \sin\delta}{\sin\beta}\begin{bmatrix} \cos(\psi-\beta)\cos\varphi\sin\delta + \sin(\psi-\beta)\sin\varphi \\ \cos(\psi-\beta)\sin\varphi\sin\delta - \sin(\psi-\beta)\cos\varphi \\ \cos\delta\cos(\psi-\beta) \end{bmatrix}. \quad (20)$$

Hence, the unit normal vector of P can be given by

$$n = \left(\frac{\partial \boldsymbol{r}}{\partial\varphi}\times\frac{\partial \boldsymbol{r}}{\partial\emptyset}\right)\Big/\left\|\frac{\partial \boldsymbol{r}}{\partial\varphi}\times\frac{\partial \boldsymbol{r}}{\partial\phi}\right\| = \begin{bmatrix} -\sin(\psi-\beta)\cos\varphi\cos\delta + \cos(\psi-\beta)\sin\varphi \\ -\sin(\psi-\beta)\sin\varphi\sin\delta - \cos(\psi-\beta)\cos\varphi \\ -\sin(\psi-\beta)\cos\delta \end{bmatrix}. \quad (21)$$

The first fundamental form is formulated as

$$I = Ed\varphi^2 + 2Fd\varphi d\phi + Gd\phi^2 \quad (22)$$

where

$$E = \frac{\partial \boldsymbol{r}}{\partial\varphi}\cdot\frac{\partial \boldsymbol{r}}{\partial\varphi} = \rho^2\sin^2\psi\cos^2\delta, \quad (23)$$

$$F = \frac{\partial \boldsymbol{r}}{\partial\varphi}\cdot\frac{\partial \boldsymbol{r}}{\partial\emptyset} = 0, \quad (24)$$

and

$$G = \frac{\partial \boldsymbol{r}}{\partial\emptyset}\cdot\frac{\partial \boldsymbol{r}}{\partial\emptyset} = \frac{\rho^2\sin^2\delta}{\sin^2\beta}. \quad (25)$$

$F = 0$ means that the iso-parametric curves, more precisely the φ-curve and ϕ-curve shown in Figure 5, are mutually orthogonal anywhere on the tooth surface Σ. Thus, the iso-parametric curves are the principal curve lines, and the base vectors coincide with the principal directions.

Yet another important conclusion is hidden behind the first fundamental form of the tooth surface; i.e., the angle β' between the tangent vector and its radius vector of ϕ-curve at any point P is always equal to β because

$$\cos\beta' = r\cdot\left(\frac{\partial \boldsymbol{r}}{\partial\phi}\right)\Big/\left\|\boldsymbol{r}\cdot\left(\frac{\partial \boldsymbol{r}}{\partial}\emptyset\right)\right\| = \cos\beta. \quad (26)$$

This conclusion implies that every ϕ-curve is a spatial logarithmic spiral curve. In comparison with the c curve, the basic differences are the cone angle γ and its initial point P_0. Based on the spherical triangle sine theorem, it is easy to obtain the relation between δ and γ. In other words,

$$\sin\delta = \sin\gamma\cos\alpha \quad (27)$$

where α is an instantaneous pressure angle. If γ is equal to the pitch angle γ_p, then α is the nominal pressure α_n, of which the typical value is 20° in gear transmission.

4.2 Second fundamental form

Differentiate the normal vector Eq. (21) with parameters φ and ϕ, and obtain the following formulas

$$\frac{\partial \boldsymbol{n}}{\partial\varphi} = \cos\delta\begin{bmatrix} \cos(\psi-\beta)\cos\varphi\cos\delta \\ \cos(\psi-\beta)\sin\varphi\cos\delta \\ -\cos(\psi-\beta)\sin\delta \end{bmatrix} \quad (28)$$

$$\frac{\partial \boldsymbol{n}}{\partial\varphi} = \sin\delta\begin{bmatrix} \cos(\psi-\beta)\cos\varphi\sin\delta + \sin(\psi-\beta)\sin\varphi \\ \cos(\psi-\beta)\sin\varphi\sin\delta - \sin(\psi-\beta)\cos\varphi \\ \cos(\psi-\beta)\cos\delta \end{bmatrix}. \quad (29)$$

The second fundamental form is given by

$$II = Ld\varphi^2 + 2Md\varphi d\phi + Nd\phi^2 \quad (30)$$

where

$$L = -\frac{\partial \boldsymbol{r}}{\partial\varphi}\cdot\frac{\partial \boldsymbol{n}}{\partial\varphi} = -\rho\sin\psi\cos(\psi-\beta)\cos^2\delta, \quad (31)$$

$$M = -\frac{\partial \boldsymbol{r}}{\partial\emptyset}\cdot\frac{\partial \boldsymbol{n}}{\partial\varphi} = -\frac{\partial \boldsymbol{r}}{\partial\varphi}\cdot\frac{\partial \boldsymbol{n}}{\partial\emptyset} = 0, \quad (32)$$

and

$$N = -\frac{\partial \boldsymbol{r}}{\partial\emptyset}\cdot\frac{\partial \boldsymbol{n}}{\partial\emptyset} = -\frac{\rho\sin^2\delta}{\sin\beta}. \quad (33)$$

In the second fundamental form, we focus on the principal curvatures and directions distribution on the tooth surface. Since $F = 0$ and $M = 0$, the principal curvature expressions can be derived respectively as

$$k_1 = \frac{L}{E} = -\frac{\cos(\psi-\beta)}{\rho\sin\psi} \quad (34)$$

and

$$k_2 = \frac{N}{G} = -\frac{\sin\beta}{\rho}. \quad (35)$$

From Eqs. (19)-(20), the principal directions can be depicted as

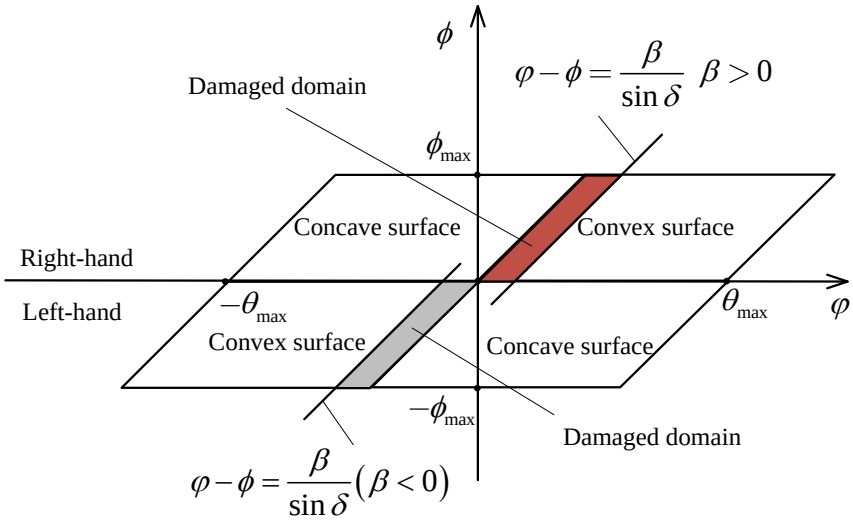

Figure 8. Pattern draft limitation for precision forging.

$$\boldsymbol{e}_1=\begin{bmatrix}cos\,\varphi\,cos\,\delta\\ sin\,\varphi\,cos\,\delta\\ -sin\,\delta\end{bmatrix} \tag{36}$$

and

$$\boldsymbol{e}_2=\begin{bmatrix}cos(\psi-\beta)\,cos\,\varphi\,sin\,\delta+sin(\psi-\beta)\,sin\,\varphi\\ cos(\psi-\beta)\,sin\,\varphi\,sin\,\delta-sin(\psi-\beta)\,cos\,\varphi\\ cos\,\delta\,cos(\psi-\beta)\end{bmatrix}. \tag{37}$$

The above explicit expressions allow us to compute the secondary characteristics of the tooth surface accurately from the gear parameters. On the other hand, we cannot accurately determine the principal curvatures and principal directions if the tooth surface is approximated by NURBS.

5. Manufacturability analysis

In the traditional cutting process, it is not possible to produce logarithmic spiral bevel gears, since the milling or hobbing will inevitably change the spiral angle during the movement of the machine tools. However, a suitable method for manufacturing logarithmic spiral bevel gears remains uncertain.

5.1 Precision forging

Among the various plastic forming methods, precision forging offers the possibility of obtaining high quality parts. It allows better material utilization in comparison to cutting, a reduction of the costs due to the shorter cycle times, and new possibilities concerning the tooth surface geometry of the forged gears. Precision forging also contributes to fulfill the demand of the production of highly loaded and small module gears widely used in the automobile industry, because of the fiber orientation which is favorable for carrying high oscillating loads [20].

However, precision forging technology is typically only applied for manufacturing spur gears and straight bevel gears [16]. For logarithmic spiral bevel gears, the basic limitation is the pattern draft of the forging die. The die geometry is obtained for logarithmic spiral bevel gears from their theoretical geometry; the manufacturability can thus be analyzed according to the above mentioned tooth surface geometry.

A suitable pattern draft along the *z*-axis, of which the unit vector $\boldsymbol{v}_d$ is (0,0,1), must satisfy

$$\boldsymbol{n}\cdot v_d\le 0 \tag{38}$$

where $\boldsymbol{n}$ is the unit normal vector of the tooth surface. For the convex tooth surface, according to Eq. (20) and Eq. (38), the following formula must work.

$$\varphi-\phi\ge\frac{\beta}{sin\,\delta} \tag{39}$$

Eq. (39) shows it is impossible to remove the forged part from the forging die without any damage if the shape of the theoretical convex tooth surface has not been modified, as seen in the parametric domain shown in Figure 8. Eq. (39) also implies that precision forging technology is only suitable for manufacturing spiral bevel gears with a smaller spiral angle. However, according to the shape modification of the damaged domain and optimization of the contact zone by TCA or the function-oriented active design method, it is en-

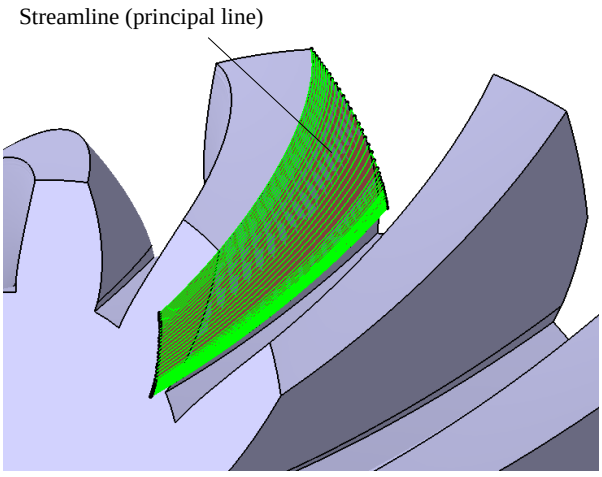

Figure 9. Streamline field orientation.

tirely possible to manufacture logarithmic spiral bevel gears using precision forging technology.

For the concave surface, the normal vector ***n*** should be reversed according to the parametric direction. Thus,

$$\varphi - \phi \le \frac{\beta}{\sin\delta} \tag{40}$$

always exists due to $-\theta_{max} \le \varphi - \phi \le 0$ $(\beta > 0)$ or $0 \le \varphi - \phi \le \theta_{max}$ $(\beta < 0)$. Thus, it is not necessary to modify the shape of theoretical concave tooth surface, as shown in Figure 8.

5.2 Multi-axis freeform milling

In terms of the manufacturing process, in almost all works it is assumed that the gears are machined using special types of machine tools, such as CNC based hobbing and milling machines. However, the kinematic structure and dynamics behavior of the CNC based gear manufacturing machine tools still inherently differ from the industrial multi-axis milling machine tools. Although freeform milling by widely used industrial multi-axis machines has an obviously lower production rate than cutting using special types of machine tools for spiral bevel gear manufacturing, in single piece and small batch productions, it is advantageous to have a broad range of size change due to unnecessary equipment investment, especially in the manufacture of substantially large gears with diameters of over 1,000 mm.

Similar to the method used for manufacturing integral impellers, tool path planning is the key to obtaining successful results for logarithmic spiral bevel gears with multi-axis freeform milling. Besides tool interference, we particularly focus on the curvature field of the tooth surface coupled with the tool path. The tooth surface geometry (in particular its principal curvature field), deeply influences its contact mechanical properties. An unsuitable tool path will damage its streamline field orientation; the tool path should thus coincide with one of the principle curvature lines of the tooth surface. More precisely, the tooth path should be ϕ-curve, since ϕ-curve is also a principal curvature line, as shown in Figure 9.

6. Conclusions

- The tooth surface of logarithmic spiral bevel gears is a parametric surface defined on a parallelogrammic domain. It undoubtedly offers many advantageous geometrical characteristics by differential geometry analysis. Analyzing the tooth surface geometry helps us to fully understand its manufacturability and possible kinematic and dynamic behavior in application.
- Because logarithmic spiral bevel gears cannot be manufactured using traditional hobbing and milling machines, analysis is carried out on their manufacturability with precision forging and multi-axis freeform milling technology. The result shows that tooth surface shape modification is inevitable for precision forging. However, tooth shape modification can be easily controlled by two simple feature parameters. In addition, the curvature streamline should be maintained for multi-axis freeform milling to obtain a high quality tooth surface.
- In theory, the truly conjugate spiral gears have a line contact. More precisely, the line contact is a spatial logarithmic spiral. However, in order to decrease the sensitivity of the gear pair to errors in tooth surfaces and to the relative positions of the mating members, a set of carefully chosen modifications must be applied to the teeth of one or both mating gears. As a result of these modifications, the logarithmic spiral bevel pair becomes mismatched, and a point contact replaces the theoretical line contact. Regardless of the method used to manufacture the mismatched logarithmic spiral bevel gears, such as precision forging and general multi-axis freeform milling, the emergent practice challenge is how to generate the optimal tooth surfaces of the pinion and the gear in order to reduce transmission error.

Acknowledgments

The research described in this paper was financially supported by the National Natural Science Foundation of China (Grant No. 61003122), and the Research Fund for Scientific and Technological Projects of Chongqing (Grant No. 2012ggB40003 and cstc2012ggB60001).

References

[1] Ai-daccak MJ, Angeles J, González-palacios MA. Modeling of bevel gears using the exact spherical involute. ASME Journal of Mechanical Design. 1994; 116(2): 364-368.

[2] Park NG, Lee HW. The spherical involute bevel gear: its geometry, kinematic behavior and standardization. Journal of Mechanical Science and Technology. 2001; 25(4): 1023-1034.
[3] Lin Y, Ren SN, Wang ZY, Zhang P. Research on spiral bevel gear tooth surface reconstruction based on NURBS. Applied Mechanics and Materials. 2012; 130: 701-705.
[4] Zhang JH, Fang ZD, Wang C. Digital simulation of spiral bevel gears' real tooth surfaces based on non-uniform rational B-spline. Journal of Aerospace Power. 2009; 24(7): 1672-1676.
[5] Su ZJ, Wu XT, Mao SM, Li JG. Design of hypoid gear tooth surface represented by non-uniform rational B-spline polynomial. Journal of Xi'an Jiaotong University. 2005; 39(1): 17-20.
[6] Tang JY, Pu TP, Dai J. Accurate modeling method of a SGM—manufactured spiral bevel gear. Journal of Mechanical Transmission. 2008; 32(1): 43-46, 83.
[7] Simon V. Optimal machine tool setting for hypoid gears improving load distribution. ASME Journal of Mechanical Design. 2001; 123(12): 577-582.
[8] Litvin FL, Zhang Y, Handschuh RF. Local synthesis and tool contact analysis of face-milled spiral bevel gears. Cleveland, OH: NASA Lewis Research Center (US); 1991 Jan. 176 p. Report No.: CR-4342.
[9] Litvin FL, Fuentes A. Gear geometry and applied theory. 2nd ed. Cambridge (NY): Cambridge University Press; 2004. 800 p.
[10] Cao XM, Fang ZD, Zhang JL. Function-oriented active tooth surface design of spiral bevel gear. Chinese Journal of Mechanical Engineering. 2007; 43(8): 155-158.
[11] Tang JY, Lu YF, Zhou C. Error tooth contact analysis of spiral bevel gears transmission. Chinese Journal of Mechanical Engineering. 2008; 44(7): 16-23.
[12] Liu GL, Fan HW. Pinion tooth surface generation strategy of spiral bevel gears. Chinese Journal of Mechanical Engineering. 2012; 25(4): 753-759.
[13] Huston RL, Coy JJ. Ideal spiral bevel gears–a new approach to surface geometry. ASME Journal of Mechanical Design. 1981; 103(4): 126-132.
[14] Tsai YC, Chin PC. Surface geometry of straight and spiral bevel gears. Transaction of the ASME. Journal of Mechanisms, Transmissions, and Automation in Design. 1987; 109: 443-449.
[15] Li Q, Wei ZL, Yan HB. A new method of constructing tooth surface for logarithmic spiral bevel gear. Applied Mechanics and Materials. 2011; 86: 399-402.
[16] Fuentes A, Iserte-Vilar JL, Gonzalez-Perez I, Sanchez-Marin FT. Computerized design of advanced straight and skew bevel gears produced by precision forging. Computer Methods in Applied Mechanics and Engineering. 2011; 200(29-32): 2363-2377.
[17] Suh SH, Jih WS, Hong HD, Chung DH. Sculptured surface machining of spiral bevel gears with CNC milling. International Journal of Machine Tools & Manufacture. 2001; 41(6): 833-850.
[18] Shunmugam MS, Rao BS, Jayaprakash V. Establishing gear tooth surface geometry and normal deviation part II-bevel gears. Mechanism and Machine Theory. 1998; 33(5): 525-534.
[19] Xia DL. The generation principle of the equiangular conic helix and the drawing of its projective view. Journal of Hefei University of Technology. 1990; 13(3): 99-105.
[20] Doege E, Nägele H. FE simulation of the precision forging process of bevel gears. CRIP Annals–Manufacturing Technology. 1994; 43(1): 241-244.